



# Application note

# All-Solid-State Battery Testing up to 407 MPa using the CompreFrame



#### Introduction

Pressure application is crucial in the testing of solid-state battery cells and materials. First, the solid electrolyte (and any active material layers) must undergo densification to form a pellet with consolidated particles [1]. Applying an insufficient densification pressure results in residual voids that are detrimental to ion transport and that can serve as nucleation points and propagation for lithium metal [2]. pathways Furthermore, the pressure applied during a measurement (e.g. charge/discharge cycling) is a key parameter also for a fully densified sample, as it influences the ionic conductivity, contact resistance, capacity retention, cycle life, lithium plating quality, etc. [1, 2]. Hence, for reproducible results, it is imperative to be able to control and monitor the pressure applied to solid-state battery cells during fabrication and testing.

The CompreFrame [3] is a spring-loaded pressure application frame for solid-state battery research. With the recent release of a 10 mm diameter piston option for the CompreCell DP [4], it is possible to apply up to 407.4 MPa (32 kN) to the sample in this setup. Since this pressure is sufficient to fully densify many solid electrolytes, both the fabrication and testing can be done in situ in the CompreFrame, with its precise pressure control and monitoring options. Specifically, it is not necessary to use a hydraulic press, which might be less accurate and without any possibility to record the pressure data. To achieve even higher pressures, a cell with 6 mm diameter pistons is available, as well as the CompreDrive system that can apply up to 75 kN [5].

In this application note, we take advantage of the new CompreCell 10 DP in the CompreFrame and demonstrate characterization of two cells with  $LiNi_{0.6}Mn_{0.2}Co_{0.2}O_2$  (NMC) cathode, graphite anode, and an Li<sub>6</sub>PS<sub>5</sub>CI (LPSCI) electrolyte: One in two-electrode mode, and three-electrode one in incorporating a lithium metal reference Twoelectrode. and three-electrode charge/discharge cycling as well electrochemical impedance spectroscopy (EIS) is shown.

## **Experimental**

The all-solid-state battery stacks were assembled in a CompreCell 10 DP cell [4] (rhd instruments GmbH & Co. KG), which has a 10 mm Ø sample cavity in a PEEK sleeve (Figure 1). For the two-electrode cell, LPSCI (79 mg;  $100 \text{ mg/cm}^2$ , Ampcera Argyrodite, MSE Supplies) was pressed into the sleeve by applying 100 MPa for 5 minutes in a ComPrep [6]. For the three-electrode cell, a gold-plated tungsten wire (25  $\mu$ m Ø, Goodfellow) was inserted into the sleeve, to be used as the basis for the reference electrode [7, 8]. LPSCI was added in two steps (to both sides of the wire; 2 X 79 mg;  $2 \times 100 \text{ mg/cm}^2$ ) and pre-compressed as described above. For both cells, NMC composite (13.5 mg;  $11.2 \text{ mg}_{NMC}/\text{cm}^2$ ; 65% (m/m) NMC622 (BASF), 32% (m/m)



LPSCI, 3% (m/m) C65 (Timcal)) was added to one side of the electrolyte pellet and graphite composite (13.5 mg; 11.7 mg<sub>Graphite</sub>/cm<sup>2</sup>; 68% (m/m) natural graphite (918-II, MTR), 32% (m/m) LPSCI) was added to the other side. The active materials were contacted directly by tungsten carbide pistons (Figure 1). The assembly and pre-compression were done in an argon-filled glove box. Once sealed, the cells are air-tight and can be operated under ambient conditions.



**Figure 1**. Sketch of the components comprising the three-electrode cell stack.

The cell temperature and pressure were controlled by a CompreFrame equipped with an HC-Addon (rhd instruments GmbH & Co. KG) [9]. All measurements were performed at 25 °C and 400 MPa unless otherwise stated.

SP-200 Biologic potentiostat for all galvanostat was used electrochemical measurements. The lithium reference electrode was created in situ by lithiating the W/Au wire as described previously [8]. Charge/discharge cycling was performed with a constant current (CC) of C/10 (based on a nominal capacity of 200 mAh/ $g_{NMC}$ ) between 3.0 V and 4.2 V cell voltage, which for the charge step was followed by a constant cell voltage (CV) stage (C/50 cutoff). EIS was performed with a peak-to-peak amplitude of 30 mV at 3 MHz – 100 Hz for the two-electrode cell and at 3 MHz – 100 mHz for the three-electrode cell (the graphite counter electrode spectra are limited to 200 kHz). The impedance data was evaluated by equivalent circuit fitting in RelaxIS 3.0 (rhd instruments GmbH & Co. KG). The figures in this application note were created using Edelweiss 0.1 (rhd instruments GmbH & Co. KG).

#### Results and Discussion

By recording impedance spectra while applying increasingly high pressures to the two-electrode cell in the CompreFrame, the effect of the initial densification of the cell stack can be monitored in situ (Figure 2). The equivalent circuit shown in Figure 2 was used to fit the spectra since the anode and cathode were still in the pristine state. The series resistance decreased with the densification pressure (visible as a shift to the left) until levelling off around 400 MPa, as observed previously for this electrolyte [10]. Furthermore, the bulk capacitance increased with the pressure (visible as a shortening of the capacitive "tail"), as the contact area of the deforming particles with the current collectors increased. In this way, precise pressure application aids in determining the required conditions for reproducible densification.



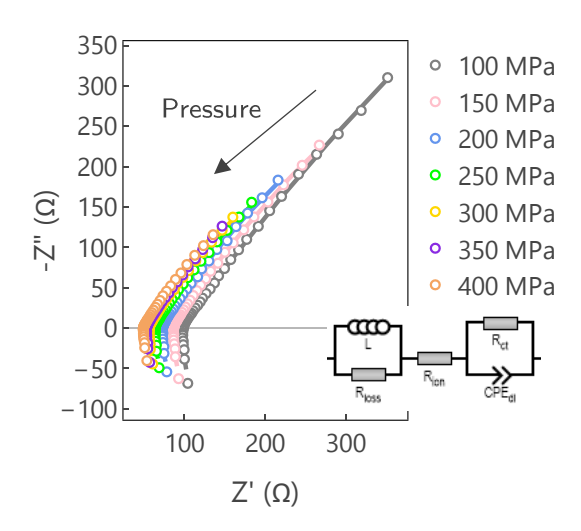


**Figure 2.** Impedance spectra of the pristine NMC/LPSCI/Graphite two-electrode cell during the initial densification. Lines indicate fits of the equivalent circuit shown.

Charge/discharge cycling the cell at 400 MPa (Figure 3) revealed an initial coulombic efficiency of 73.9% and coulombic efficiency of subsequent cycles above 96%. The cycle-to-cycle discharge capacity retention was 98.5% - 99.5%.

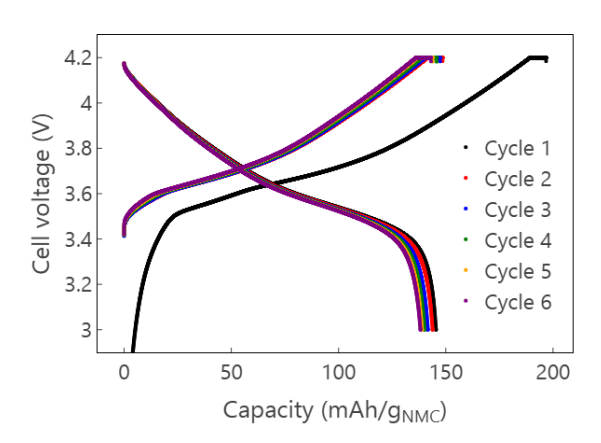


**Figure 3.** Charge/discharge curves for the NMC/LPSCI/Graphite two-electrode cell.

For the three-electrode cell, the reference electrode first had to be formed through *in situ* lithiation by passing a reductive

current of 5  $\,\mu A$  for 30 min, as described in more detail elsewhere [8]. The cell was then subjected to charge/discharge cycling, and it was discovered that the lithium reference electrode potential started to drift already during the second cycle, likely due to a reaction between the lithium metal and the electrolyte. This manifests as both the anode and cathode potentials decreasing in unison (not shown), and can be remedied by plating additional lithium metal on the reference electrode [7]. In this way, the reference electrode will have a larger lithium reservoir, and the potential will be stable even when the electrolyte has some reactivity towards lithium metal. Hence, the reference electrode was lithiated for another 2 hours, after which the five charge/discharge cycles shown in Figure 4 were recorded. In this condition, the reference electrode potential stable for at least one week.

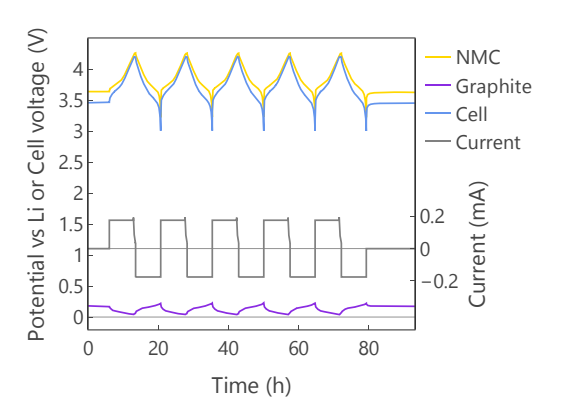


**Figure 4.** Charge/discharge curves for the NMC/LPSCI/Graphite three-electrode cell (lithium metal reference electrode) at C/10.

The individual potentials of the NMC cathode and the graphite anode during cycling can be disambiguated in the three-



electrode cell (Figure 4). This gives more specific information about the anode and cathode reactions, and the interplay between them during cell cycling. For example, it is evident that the NMC cathode was the limiting electrode in this cell (as intended), since that was the electrode hitting the potential limits (black line in Figure 4), while the graphite anode cycled in a more restricted potential region, never reaching extreme values (red line in Figure 4). It is also interesting to note that since during the CV stage, the cell voltage is kept constant (not the individual electrode potentials), the anode cathode potentials shift depending on their relative impedances. In this case, the potentials of both electrodes vs Li increased by about 20 mV during the CV stage.

In addition to the full cell spectra, the individual spectra for each electrode are also accessible for the three-electrode cell, shown for 0% state of charge (SOC) in Figure 5b. The charge transfer as well as the diffusion process is clearly separated into the NMC and graphite contributions. The main contributor to both the charge transfer and the solid-state diffusion in this case was the NMC cathode, so to quantify the parameters of the graphite processes in the full cell, a reference electrode is necessary.

The full cell spectrum can also be reconstructed from the individual electrode spectra: The sum of the cathode and anode spectra completely overlaps the two-electrode spectrum (not shown) except at the highest frequencies (>100 kHz) where

the difference in the physical cell connections lead to a different inductive contribution.

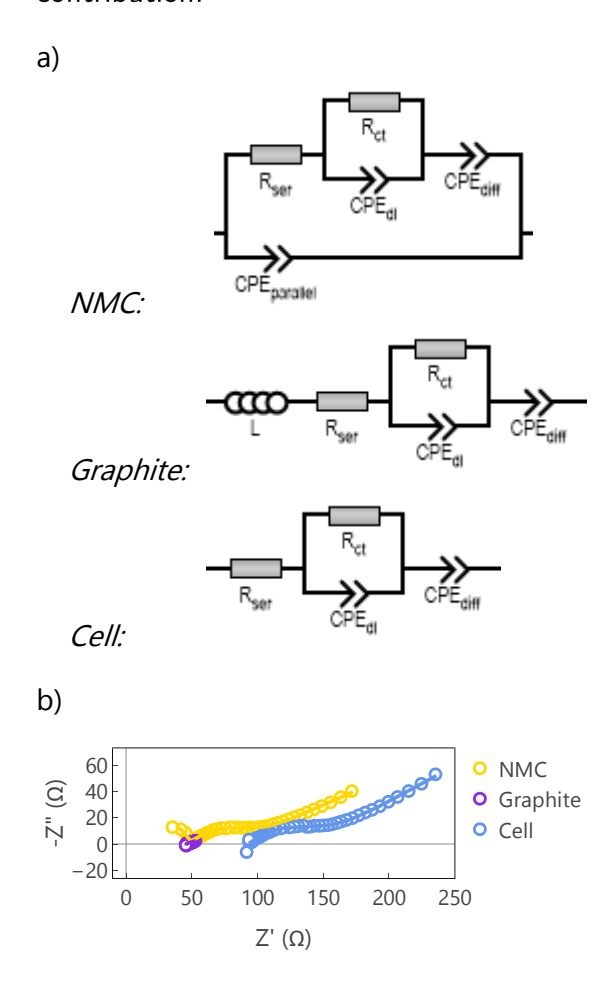
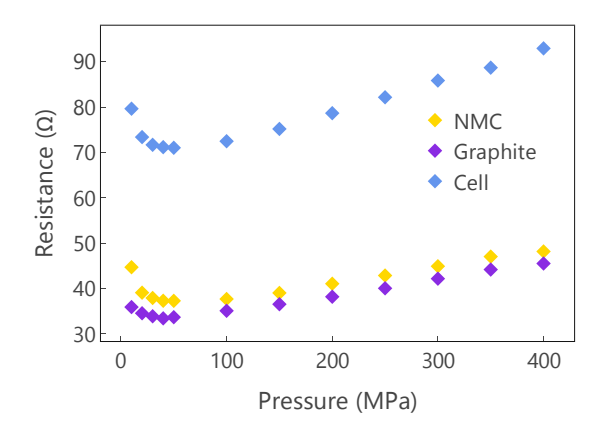


Figure 5. a) Equivalent circuits used to fit the three-electrode spectra. b) Individual EIS spectra of each electrode as well as the full NMC/LPSCI/Graphite cell (after cycling, 0% SOC). Lines indicate fits of the respective equivalent circuits.

After the cycling at 400 MPa, the pressure was released in steps down to 10 MPa, with EIS recorded at each pressure. Fitting the equivalent circuits shown in **Figure 5a** to the spectra reveals *i.a.* how the series resistance ( $R_{ser}$ ) for each electrode varies with pressure (**Figure 6**).  $R_{ser}$  is the sum of the ionic resistance ( $R_{ion}$ ) of the solid



electrolyte (between that electrode and the reference electrode) and the contact resistance with the current collector  $(R_{con})$ . At high pressures (>100 MPa),  $R_{ser}$ increased linearly with pressure for both electrodes, since the solid electrolyte lattice can elastically contract, thus restricting ion flow. The slope of  $R_{ion}$  vs pressure is related to the so-called activation volume of the electrolyte [1, 10]. Note that this behavior opposite to that of the initial densification process (Figure 2), since in that case, the effect of the plastic consolidation of electrolyte particles completely eclipses that of the elastic lattice deformation.



**Figure 6.** Series resistance of each electrode as well as the full NMC/LPSCI/Graphite cell while releasing the pressure after cycling (0% SOC).

At lower pressures,  $R_{ser}$  decreased with pressure, with a shallow minimum around 40 MPa, since  $R_{con}$  then became significant. The exact pressure range at which this occurs will be different depending on the materials of the cell as well as the current collectors, but in this case the optimum pressure to apply during

measurements, in order to maximize the ionic conductivity, is 30 - 100 MPa. This highlights the importance of accurate pressure control and monitoring during both densification and cycling to achieve reproducibility between cells.

### Summary

The capabilities of a new CompreCell DP with 10 mm diameter pistons were demonstrated in the CompreFrame pressure application frame using two NMC|LPSCI|Graphite solid-state battery cells, with and without a lithium metal reference electrode, respectively. In this setup, it is possible to apply up to 407.4 MPa, enabling full densification, without the use of an external press. The effect of pressure on the impedance during and after densification was investigated. Charge/discharge cycling at 400 MPa is also shown in two- and three-electrode mode. The ability to precisely control the pressure is crucial to achieving reproducible fabrication and measurement conditions.

#### Literature

[1] C. Schneider, C. P. Schmidt, A. Neumann, M. Clausnitzer, M. Sadowski, S. Harm, C. Meier, T. Danner, K. Albe, A. Latz, W. A. Wall and B. V. Lotsch, "Effect of Particle Size and Pressure on the Transport Properties of the Fast Ion Conductor



- t-Li7SiPS8," *Advanced Energy Materials*, vol. 13, no. 15, p. 2203873, 2023.
- [2] T. Krauskopf, F. H. Richter, W. G. Zeier and J. Janek, "Physicochemical Concepts of the Lithium Metal Anode in Solid-State Batteries," *Chemical Reviews*, vol. 120, no. 15, p. 7745, 2020.
- [3] rhd instruments GmbH & Co. KG, "CompreFrame," October 2025. [Online]. Available: https://rhd-instruments.de/solutions-and-products/for-solid-state-batteries/compreframe/.
- [4] rhd instruments GmbH & Co. KG, "CompreCell DP," October 2025. [Online]. Available: https://rhd-instruments.de/solutions-and-products/for-solid-state-batteries/comprecell-dp/.
- [5] rhd instruments GmbH & Co. KG, "CompreDrive," October 2025. [Online]. Available: https://rhd-instruments.de/solutions-and-products/for-solid-state-batteries/compredrive/.
- [6] rhd instruments GmbH & Co. KG, "ComPrep," October 2025. [Online]. Available: https://rhd-instruments.de/solutions-and-products/for-solid-state-batteries/comprep/.
- [7] J. Hertle, F. Walther, B. Mogwitz, S. Schröder, X. Wu, F. H. Richter and J.

- Janek, "Miniaturization of Reference Electrodes for Solid-State Lithium-Ion Batteries," *Journal of The Electrochemical Society*, vol. 170, p. 040519, 2023.
- [8] C. Karlsson, "Application note: Three-Electrode All-Solid-State Battery Cycling," December 2023. [Online]. Available: https://rhd-instruments.de/magazine/three-electrode-all-solid-state-battery-cycling/.
- [9] rhd instruments GmbH & Co. KG, "HC-Addon," October 2025. [Online]. Available: https://rhd-instruments.de/solutions-and-products/for-solid-state-batteries/hc-addon/.
- [10] S. Pacetti, C. Karlsson, E. Mijit, M. Drüschler, A. D. Cicco, N. Pinto, D. Bresser and S. Rezvani, "Optimization of ionic and electronic properties of Li6PS5CI based on structural dynamics," *In preparation*, 2025.

